New Journal of Physics
The open access journal at the forefront of physics

Deutsche Physikalische Gesellschaft DPG IOP Institute of Physics

PAPER • OPEN ACCESS

Eliminating light shifts for single atom trapping

To cite this article: Nicholas R Hutzler *et al* 2017 *New J. Phys.* **19** 023007

New Journal of Physics
The open access journal at the forefront of physics

Deutsche Physikalische Gesellschaft DPG
IOP Institute of Physics

Published in partnership with: Deutsche Physikalische Gesellschaft and the Institute of Physics

CrossMark

OPEN ACCESS

RECEIVED
26 October 2016

REVISED
29 December 2016

ACCEPTED FOR PUBLICATION
18 January 2017

PUBLISHED
2 February 2017

PAPER

Eliminating light shifts for single atom trapping

Nicholas R Hutzler[1], **Lee R Liu, Yichao Yu and Kang-Kuen Ni**

Department of Chemistry and Chemical Biology, Harvard University, Cambridge, MA, 02138, United States of America
Department of Physics, Harvard University, Cambridge, MA, 02138, United States of America
Harvard-MIT Center for Ultracold Atoms, Cambridge, MA, 02138, United States of America
[1] Author to whom any correspondence should be addressed.

E-mail: hutzler@physics.harvard.edu **and** ni@chemistry.harvard.edu

Keywords: optical tweezers, atom trapping, atom cooling, single atoms, optical trapping

Abstract

Microscopically controlled neutral atoms in optical tweezers and lattices have led to exciting advances in the study of quantum information and quantum many-body systems. The light shifts of atomic levels from the trapping potential in these systems can result in detrimental effects such as fluctuating dipole force heating, inhomogeneous detunings, and inhibition of laser cooling, which limits the atomic species that can be manipulated. In particular, these light shifts can be large enough to prevent loading into optical tweezers directly from a magneto-optical trap. We implement a general solution to these limitations by loading, as well as cooling and imaging the atoms with temporally alternating beams, and present an analysis of the role of heating and required cooling for single atom tweezer loading. Because this technique does not depend on any specific spectral properties, it should enable the optical tweezer platform to be extended to nearly any atomic or molecular species that can be laser cooled and optically trapped.

1. Introduction

Interacting neutral atoms with quantum controls are a powerful platform for studies of quantum information and quantum many-body physics. Systems of individually trapped atoms [1] offer single particle control and detection with the flexibility to configure geometry and interactions in real time. This versatility has already allowed many proof-of-principle demonstrations, including quantum logic gates [2–5], single-atom photon switches [6], and quantum simulators of spin systems [4, 7]. Scaling up the complexities of such a system by increasing the number of species trapped offers exciting new directions. For example, dipolar atoms and polar molecules offer long-range, tunable, anisotropic interactions; ultracold arrays of these species with individual control would allow explorations of new strongly correlated systems and exotic quantum phases [8]. Molecules also possess many internal degrees of freedom that provide additional handles for quantum control.

One platform for realizing these applications is to confine single atoms in tight optical dipole 'tweezer' traps, where the size of the trap is of order the wavelength [1]. Since the polarizabilities of the ground and excited states are not perfectly matched, the atomic transitions will be shifted relative to their value in free space by a light shift [9]. This gives rise to a number of undesirable effects when scattering near-resonant photons, such as fluctuating dipole force heating [10, 11], where the atom sees temporal jumps in the gradient of the trapping potential as it cycles between the ground and excited state, inhibition of cooling due to the breakdown of hyperfine coupling [12, 13], and spatially varying detuning and scattering rate. Because cooling is required for efficient loading and detection, these effects can interfere with successful operation of the tweezer. Therefore, the loading of a wide variety of atomic species, each with an associated level structure, is made challenging by the effects of light shifts.

Problems related to light shifts were recognized in the pioneering days of laser cooling and trapping [14, 15], and a number of techniques were demonstrated to deal with them. One powerful method is to temporally alternate the trapping and near-resonant light, such that the atoms never scatter near-resonant photons when the trap is on, effectively eliminating light shifts. This method was used for cooling in the first realization of optically trapped bulk samples of atoms [16] and for improved detection of trapped single atoms [17–19]. In this

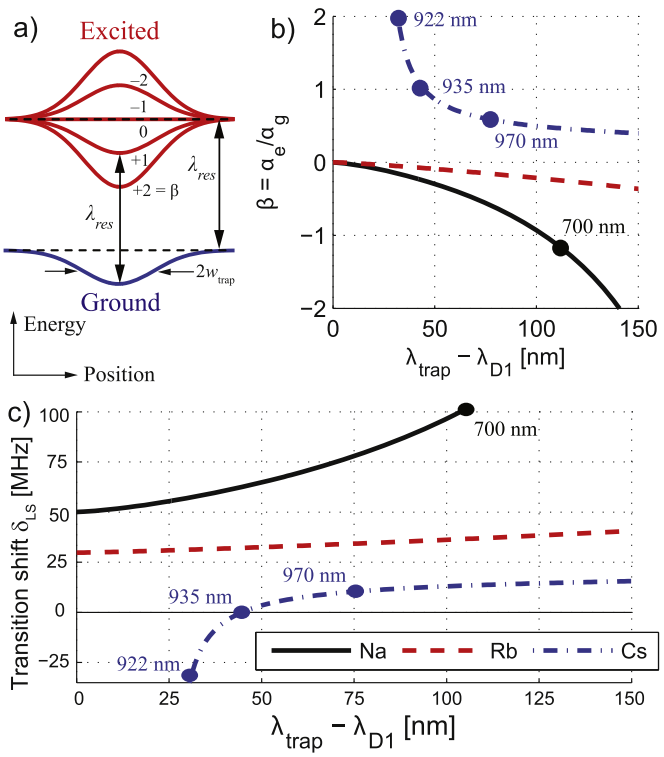

Figure 1. Light shifts in optical dipole traps. (a) An illustration of light shifts in a trap with waist w_{trap} for ground (blue) and different excited state potentials (red) in terms of the excited/ground polarizability ratio $\beta = \alpha_e/\alpha_g$. For $\beta < 1$ ($\beta > 1$) the atom will see resonant light of wavelength λ_{res} become red-shifted (blue-shifted) upon entering the trap. (b) The polarizability of the $m_j = 3/2$ manifold [24] for selected alkalis. The $D1$ transition wavelengths λ_{D1} for Na, Rb, and Cs are 590 nm, 795 nm, and 895 nm, respectively. (c) A comparison of light shifts on the cycling transition with trap depth 10 T_{Doppler}, following [24]. Transition light shift δ_{ls} is defined as the change in the transition frequency relative to free space; a positive shift means that the energy splitting between the ground and excited states increases (e.g. $\beta = -1$).

manuscript, we load single atoms of cesium (Cs) and sodium (Na) from magneto-optical traps, and demonstrate the effectiveness of modulation when applied to single atom traps where the conventional loading method [1] fails due to light shifts. We additionally implement this technique for cooling and detection of single atoms to shed light on the loading, cooling, and detection processes. We expect this technique will enable single atom and molecule loading of tweezers of essentially any species that can be laser-cooled and optically trapped, in particular exotic species such as polar molecules and dipolar atoms [8].

2. Light shifts and single atom traps

We investigate using Na and Cs atoms in optical tweezers in an apparatus that follows the general approach of [1, 20, 21]. A collimated, red-detuned laser beam is incident on a 0.55 NA objective that creates a diffraction-limited, sub-micron tweezer. The wavelength ranges used are 895–980 nm for Cs, and 700 nm for Na. The focus of the objective is in the center of a MOT, which provides a local high density cloud of cold atoms for loading into the tweezer. Atoms crossing the tweezer in the presence of cooling from the MOT beams may be loaded into the tweezer. Because of light-assisted collisions between the trapped atom and other atoms present in the MOT, the expected successful loading probability is around 50%–60% [1, 22], though there are techniques to increase this number by using additional lasers [23]. A dichroic mirror separates the tweezer light from fluorescence of the trapped atom, which is then focused onto a camera for detection via imaging, with an overall fluorescence collection efficiency of 4%. After loading the atom, the MOT cloud is allowed to disperse so that the atom can be imaged with a low background. Single atoms are identified by imposing a threshold of photon counts (figure 2). The same beams are used for the MOT, cooling, and detection, and will generally be referred to as the 'resonant beams'.

Due to the many electronic states in atoms, the polarizability of a given excited state, α_e, can be either positive or negative independent of the ground state polarizability, α_g [24] (figure 1(a)). We define the wavelength-dependent ratio of polarizabilities as $\beta \equiv \alpha_e/\alpha_g$. Note that in addition to the scalar component common to all the Zeeman levels within a hyperfine state, there are also vector [21] and tensor components that shift the Zeeman levels relative to each other. This means that even for the special case when $\beta = 1$, a 'magic'

wavelength [25, 26], where the scalar shifts in the ground and excited states are equal, the Zeeman sublevels in the atom will generally still experience a differential shift. Any light shifts can prevent loading of the atoms, and we will focus on a method the eliminates all light shifts from the loading process; therefore, for the majority of the manuscript, the distinction between them is not crucial and we will generally discuss only the (simpler) scalar light shift.

In figures 1(b) and (c), we calculate light shifts for Cs and Na (and Rb for comparison) in the presence of a red-detuned tweezer of depth 10 $T_{\mathrm{dopp}} \sim$ 1–3 mK, where T_{dopp} is the Doppler temperature, for a range of trapping wavelengths. For Cs atoms in the range of ~930–970 nm, the light shifts are small, and are near zero ($\beta \approx 1$) at 935 nm. For Na atoms over a large range of experimentally convenient wavelengths (630–1064 nm), $\beta < 0$. Combined with the higher Doppler temperature of Na, this results in a large light shift that reduces the photon scattering rate and prevents the cooling that is required to capture the atom. Furthermore, the light shift is comparable to the excited state hyperfine splitting of ≈60 MHz and inhibits sub-Doppler cooling due to the breakdown of hyperfine coupling [12, 13]. Finally, attempting to load the atom from a MOT, where the excited-state fraction is typically ~25%, an anti-trapped excited state will reduce the average trap depth, therefore requiring higher intensity and resulting in even larger light shifts and fluctuating dipole forces.

To circumvent issues related to loading, heating, and detection that result from light shifts, we alternate the trapping and cooling light such that they are never on at the same time. Specifically, we modulate the intensities of the tweezer and resonant light as square waves with frequencies between 1 and 3 MHz. The fast modulation technique works well as long as the trap modulation frequency f_{mod} is much greater than twice the trap frequencies, so the atom does not suffer from parametric heating [27], yet still experiences a trap given by the time-averaged intensity. Typical (axial, radial) trap frequencies are $\approx 2\pi \times (12,\ 71)$ kHz for Cs, and $\approx 2\pi \times (80,\ 500)$ kHz for Na. In addition, we require $f_{\mathrm{mod}} \lesssim \gamma/2\pi$, where γ is the natural linewidth, so that the atom will have enough time to decay into the ground state before the trapping light is switched back on.

The modulation is realized by using the first order diffracted beam from an acoustic-optical modulator driven by an 80 MHz sine wave mixed with the modulating square wave. The resonant beams have 50% duty cycle[2], and the tweezer has 30%–40% duty cycle to minimize overlap with the resonant light. With this technique, single atoms were successfully loaded into a tweezer from a MOT or an optical molasses ($T \approx$ 10–30 μK). An image of a single Na atom and a histogram of photoelectron counts on the CCD camera from repeated loading attempts using the modulation technique is shown in figure 2(a). We note that, in the absence of the modulation technique, we were not able to observe loading of a single Na atom from a MOT or molasses into a diffraction-limited tweezer[3] after varying a wide range of parameters including tweezer depth, wavelength, MOT cooling power, repump power, detuning, and magnetic field gradient.

3. Measuring and controlling light shifts

To illustrate the robustness of fast modulation and the detrimental effects of light shifts, we vary the relative phase of the resonant light and tweezer modulation and measure the probability of loading an atom in figure 2(b). When the tweezer and resonant light are not on at the same time, the atoms see no light shift but are still Doppler cooled, and we can reliably load the tweezer. On the other hand, as the tweezer and resonant light begin to overlap in time, the light shifts inhibit photon scattering and the loading suffers. We find that the center of the loading curve is not when the resonant light and tweezer are exactly out of phase (180°), but when the tweezer trails resonant light turn-off by ~30 ns (about twice the Na radiative decay lifetime of 16 ns) due to the time that the atoms spend in the excited state, as shown in the inset of figure 2(b).

To understand the roles of light shifts in loading and detection, we can study the number of photons that an atom can scatter in the tweezer versus detuning. Figure 3 shows photons scattered versus detuning δ of the imaging laser (relative to the atomic resonance in free space) for a single Cs atom in a tweezer with an imaging duration of 50 ms and an intensity of 0.3 mW cm^{-2} $\approx 0.1 I_{\mathrm{sat}}$. While illuminated with near-resonant light, the atom scatters photons at a rate that depends on the detuning from the atomic resonance [28], and experiences recoil heating due to spontaneous emission (see the appendix for additional details). Applying the modulation technique to detect single atoms gives a reference line shape that is free of light shifts (blue curve in figure 3). Let us first explain the qualitative features of this curve. For $\delta \gtrsim -\gamma/2$, no effective cooling is present and therefore only a small number of photons can be scattered before the atom is heated out of the tweezer[4]. However, if the

[2] We find that the resonant light can be modulated at all times and still yield a dense MOT with temperature $\lesssim 2T_{\mathrm{dopp}}$, and that polarization gradient cooling (PGC) with modulated beams yields temperatures similar to those achieved with unmodulated (CW) beams. The lifetime of the single atom in the tweezer is ≈5 s for both modulated and CW tweezers.

[3] We were able to load into larger tweezers with waist >1 μm with an unmodulated tweezer and MOT beams, though the loading was only a few percent efficient.

[4] With no cooling, the atom would scatter typically on the order of 100 photons before being heated out of the ≈ 1 mK tweezer.

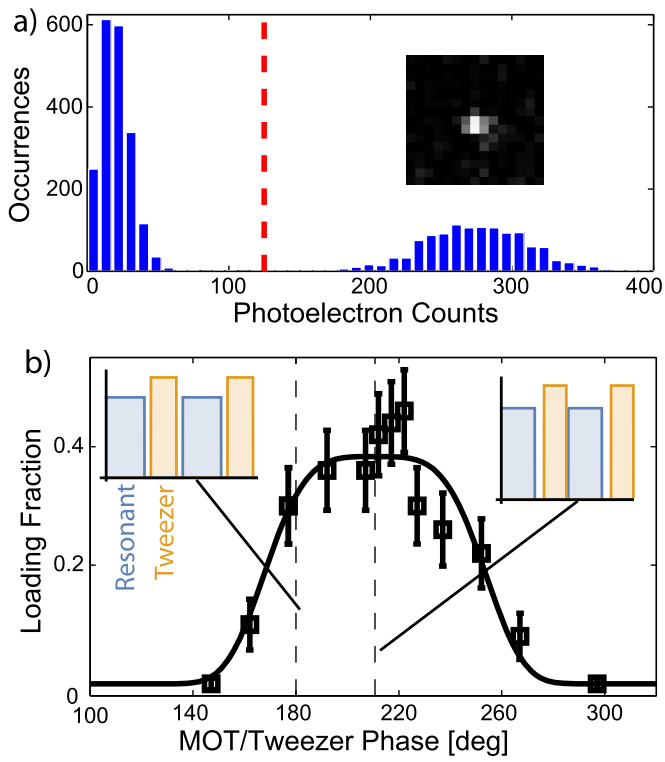

Figure 2. Single Na atom in a tweezer. (a) A histogram of photoelectron counts in a 5 × 5 region around the atom for repeated loading cycles. The cutoff (red dashed line) distinguishes between 0 and 1 atom, which are the only outcomes for this loading mechanism [1]. (Inset) An image of a single Na atom in the tweezer. (b) Single Na atom loading performance versus relative phase between MOT (resonant) and tweezer modulated intensities. When the intensities overlap, light shifts prevent loading and detection. The data shown here is for 3 MHz modulation with 50% duty cycle for the resonant light and 30% for the tweezer light intensity, respectively. The curve is to guide the eye. (Inset) Timing sequences of resonant and tweezer light at phase delays of 180° and 211° (optimum, corresponding to ~30 ns, or about twice the Na radiative decay lifetime of 16 ns).

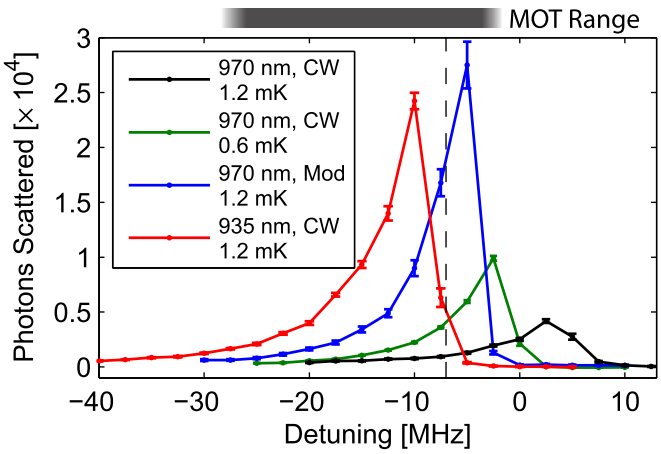

Figure 3. Scattered photons (assuming 4% detection efficiency) versus imaging detuning for single Cs atoms, with various combinations of modulated (Mod) or unmodulated (CW), 0.6 mK or 1.2 mK tweezer depths, and 970 nm ($\beta \approx 0.5$) or 935 nm ($\beta \approx 1$) tweezer wavelength. The MOT detuning is indicated by the vertical dashed line at −7 MHz. 0 MHz corresponds to the free-space atomic resonance. The line shape is explained qualitatively in the main text.

near-resonant light is red-detuned on the order of $\delta \lesssim -\gamma/2$, then Doppler and sub-Doppler cooling can keep the atom cold while it scatters photons. We find the equilibrium temperature T_{eq} is typically $\lesssim 1/4$ of T_{dopp} (with either CW or modulated beams, after optimizing), showing that sub-Doppler cooling is still occurring when modulation is implemented, though possibly limited by the disruption of the coherences required for sub-Doppler cooling [29]. Since this temperature is well below the typical depth of $U_0 \approx 1$ mK, this is sufficient for loading and as a starting point for further cooling [20], which is currently ongoing. As the detuning becomes

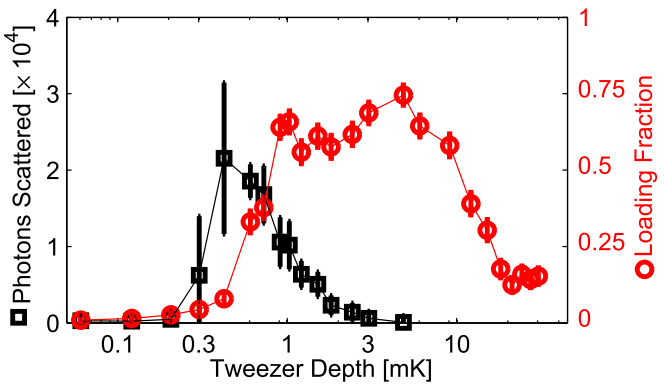

Figure 4. Photons scattered and loading probability for various CW tweezer depths. Both quantities require some minimum trap depth to allow sufficient photons to be scattered for detection. The number of photons scattered decreases with increasing depth because light shifts reduce the scattering rate while the imaging time is kept fixed. However, the loading fraction remains large as long as the scattering rate is large enough to cool the atom into the trap.

more red, the number of photons scattered is decreased due to the finite imaging time. A numerical model of the line shape is given in the appendix.

To quantify and illuminate the roles of different heating and cooling effects due to light shifts, we perform measurements with a controlled amount of light shift applied to the Cs atom by tuning the tweezer wavelengths and depths without modulation. When a light shift δ_{ls} is present, the atomic resonance shifts accordingly. In figure 3, the peaks of the 970 nm CW tweezers for two depths (black, green curves) track the δ_{ls} shift while the scattering line shapes qualitatively retain the same asymmetry—cooling on the red-detuned (left) side of the peak and heating on the blue-detuned (right) side of the peak. Furthermore, the peak number of photon scatters reduces as the light shifts increase due to fluctuating dipole force heating and inhomogeneous detuning, that is, the fact that the atom will see a range of detunings as it samples different trap depths. For $\beta \approx 1$ (magic wavelength at 935 nm, red curve), the peak photon number is similar to the no light shift case. The residual shift of the 935 nm curve is likely due to the fact that the magic wavelength is not for all hyperfine levels due to the tensor light shift.

The scattering line shapes in figure 3 not only provide information about single atom detection, but also crucially connect to single atom loading, since the conservative tweezer potential requires cooling in order to efficiently trap an atom. A numerical estimate suggests that of the order 100 photons are required to cool the atom into the trap. During single atom loading, the cooling provided by the near-resonant MOT light has a detuning that is constrained relative to the free space value (−7 MHz for Cs in our experiment) since the MOT has a constant detuning. This detuning can be adjusted to match the light shift, but is limited to a finite range for reliable MOT loading (shaded bar in figure 3).

The regimes where $\beta > 1$ and $\beta < 1$ present different challenges to atom loading. For $\beta > 1$, the atom will see the resonant beams become shifted to the blue upon entering the tweezer ($\delta_{ls} < 0$). If β is large enough such that $|\delta_{ls}| \gtrsim |\delta_{MOT}|$, this will result in significant Doppler heating, and the atom cannot be efficiently loaded directly from a MOT. We demonstrate this with Cs in a 922 nm tweezer, where $\beta \approx 2$; at this wavelength we were not able to load any single atoms using the conventional CW loading method, but achieved robust loading (~50% success rate) with fast modulation.

On the other hand, if $\beta < 1$, the atom will see the resonant light become shifted to the red in the tweezer ($\delta_{ls} > 0$). As long as this shift is not too large, Doppler cooling will continue and the atom can be loaded and detected. However, if the light shift is too large, the atom may not scatter enough photons to become deeply trapped. Na atoms with a 700 nm tweezer (β between −1 and −2 depending on hyperfine level) fall into this category as discussed prior to figure 2. Here, we demonstrate the breakdown of single Cs atom loading into a 970 nm tweezer (β between 0 and 0.5 depending on hyperfine level) as the trap depth (as well as the light shift) increases (figure 4). We also measure how many photons can be scattered at various corresponding trap depths. To eliminate variability in loading for the scattering rate measurement, we load single atoms under a fixed trap depth (≈1 mK) and ramp the tweezer to various depths for detection. Imaging intensity and duration are kept fixed. In figure 4, we see that as the tweezer becomes deeper, the scattering rate is reduced due to the light shift that increases the effective detuning of the detection light. Similarly, resonant light becomes increasingly detuned during the loading phase as the atom is cooled into the tweezer and sees an increasing light shift. For deep enough tweezers, the light shift increases so quickly that the scattering rate is turned off before the atom is effectively trapped. Because fewer photons are needed to cool (~100) compared to the number needed for high-

fidelity images (of the order 1000–10 000), the number of photons scattered falls more quickly than the loading rate as the trap depth is increased.

4. Conclusion

We present an experimental investigation the effects of light shifts in loading, cooling, and detecting single atoms in optical tweezers, and demonstrate tweezer loading from MOTs under conditions where light shifts would prevent loading via previously demonstrated methods. We robustly load both single Na and Cs atoms in tweezer traps, which provide a promising avenue to produce single polar molecules. This approach is versatile and can be applied to other interesting atomic and molecular species that can be optically trapped and cooled, which in recent years has grown to include very exciting species such as polar molecules and dipolar atoms. This could provide novel sources of cold atoms and molecules for quantum information and simulation, as well as interfacing with hybrid quantum systems.

Acknowledgments

We thank Adam Kaufman, Jeff Thompson, and Mikhail Lukin for many helpful discussions; Sebastien Garcia for feedback on the manuscript; and Yu Liu and Jessie Zhang for experimental assistance. NRH acknowledges support from Harvard Quantum Optics Center. This work is supported by the NSF through the Harvard-MIT CUA (grant PHY-1125846), as well as the AFOSR Young Investigator Program (grant FA9550-15-1-0260), the Arnold and Mabel Beckman Foundation, the Alfred P Sloan Foundation (grant FG-2015-65253), and the William Milton Fund.

Appendix. Model for photons scattered versus detuning

Consider an atom of mass m in a 1D harmonic trap of depth $U_0 \approx 1$ mK and temperature T. Expose the atom to near-resonant light of wavelength λ_{res} so that it begins to scatter photons at a rate R_{scat} given by [28]

$$R_{\mathrm{scat}} = \frac{1}{2}\frac{s_0\gamma}{1 + s_0 + (2\delta/\gamma)^2}, \tag{1}$$

where γ is the natural width, δ is the detuning from resonance including light shifts, and $s_0 = I/I_{\mathrm{sat}}$ is the saturation parameter. Let us consider the effects of Doppler heating/cooling, recoil heating, and PGC.

For $s_0 \ll 1$, the Doppler heating/cooling rate is given approximately by

$$\dot{E}_{\mathrm{dopp}} = \langle \vec{F}_{\mathrm{OM}} \cdot \vec{v} \rangle = \alpha \langle v^2 \rangle = \alpha k_B T/m, \tag{2}$$

where $\vec{F}_{\mathrm{OM}} = -\alpha\vec{v}$ is the optical molasses force, and

$$\alpha = \frac{8\hbar k^2 \delta s_0}{\gamma(1 + s_0 + (2\delta/\gamma)^2)^2}, \tag{3}$$

where $k = 2\pi/\lambda_{\mathrm{res}}$. We used the fact that $\langle v^2 \rangle = k_B T/m$ in a 1D trap. The recoil heating rate is given by

$$\dot{E}_{\mathrm{recoil}} = 4\hbar\omega_{\mathrm{recoil}} R_{\mathrm{scat}}, \tag{4}$$

where $\omega_{\mathrm{recoil}} = \hbar k^2/2m$.

To model PGC [29], we use

$$\dot{E}_{\mathrm{PGC}} \propto T\hbar k^2 \frac{\delta\gamma}{5\gamma^2 + 4\delta^2}, \tag{5}$$

with a scaling factor chosen to reproduce the observed equilibrium imaging temperature of $\approx 40\ \mu\mathrm{K} < T_{\mathrm{dopp}}$ for Cs. Including PGC is important not only to understand the sub-Doppler temperature, but also the shape of the curve shown in figure A1.

The total heating/cooling rate of the atom $\dot{E}_{\mathrm{tot}}$ is obtained by summing these contributions. We can perform a simple estimate of the total number of photons scattered with the following routine, starting with some initial temperature T_0 and initial survival probability $P_0 = 1$:

(i) Increase the temperature to $T_{i+1} = T_i + \mathrm{d}t \times \dot{E}_{\mathrm{tot}}/k_B$

(ii) Reduce the survival probability of the atom P_i to $P_{i+1} = P_i \times (1 - \mathrm{e}^{-U_0/k_B T})$, the fraction of the Boltzmann distribution that is higher than the trap depth

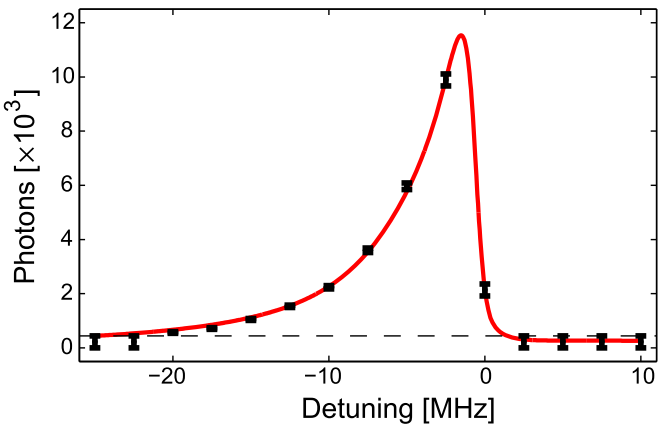

Figure A1. Fit of measured photons versus detuning curve to the model. We allow the overall height, light shift, and scaling factor on the heating/cooling rate to vary in the fit. The data is for a single Cs atom in a 970 nm tweezer trap that is 0.6 mK deep, with initial temperature of 10 μK from polarization gradient cooling before imaging, which was measured independently by release/recapture and Raman sideband thermometry. The horizontal dashed line indicates the detection limit due to background.

(iii) Repeat until $P \ll 1$.

If we use $\mathrm{d}t = 1/R_{\mathrm{scat}}$, then the total number of photons is given approximately by $\sum_i P_i$.

This approach is very simple and ignores many of the complexities of the system, but captures the important features. In particular, this model reproduces the overall shape of the photon versus detuning data and helps build understanding of the loading and imaging mechanisms.

References

[1] Schlosser N, Reymond G, Protsenko I and Grangier P 2001 *Nature* **411** 1024–7
[2] Wilk T, Gaëtan A, Evellin C, Wolters J, Miroshnychenko Y, Grangier P and Browaeys A 2010 *Phys. Rev. Lett.* **104** 010502
[3] Isenhower L, Urban E, Zhang X L, Gill A T, Henage T, Johnson T A, Walker T G and Saffman M 2010 *Phys. Rev. Lett.* **104** 010503
[4] Müller M M, Murphy M, Montangero S, Calarco T, Grangier P and Browaeys A 2014 *Phys. Rev.* A **89** 032334
[5] Kaufman A M, Lester B J, Foss-Feig M, Wall M L, Rey A M and Regal C A 2015 *Nature* **527** 208–11
[6] Tiecke T G, Thompson J D, de Leon N P, Liu L R, Vuletić V and Lukin M D 2014 *Nature* **508** 241–4
[7] Labuhn H, Barredo D, Ravets S, de Léséleuc S, Macrì T, Lahaye T and Browaeys A 2016 *Nature* **534** 667–70
[8] Baranov M A, Dalmonte M, Pupillo G and Zoller P 2012 *Chem. Rev.* **112** 5012–61
[9] Grimm R, Weidemüller M and Ovchinnikov Y B 2000 *Adv. At. Mol. Opt. Phys.* **42** 95–170
[10] Dalibard J and Cohen-Tannoudji C 1985 *J. Opt. Soc. Am.* B **2** 1707
[11] Alt W 2004 Optical control of single neutral atoms *PhD Thesis* Bonn
[12] Haller E, Hudson J, Kelly A, Cotta D A, Peaudecerf B, Bruce G D and Kuhr S 2015 *Nat. Phys.* **11** 738–42
[13] Neuzner A, Körber M, Dürr S, Rempe G and Ritter S 2015 *Phys. Rev.* A **92** 053842
[14] Gordon J P and Ashkin A 1980 *Phys. Rev.* A **21** 1606–17
[15] Dalibard J, Reynaud S and Cohen-Tannoudji C 1983 *Opt. Commun.* **47** 395–9
[16] Chu S, Bjorkholm J E, Ashkin A and Cable A 1986 *Phys. Rev. Lett.* **57** 314–7
[17] Johnson T A, Urban E, Henage T, Isenhower L, Yavuz D D, Walker T G and Saffman M 2008 *Phys. Rev. Lett.* **100** 113003
[18] Shih C Y and Chapman M S 2013 *Phys. Rev.* A **87** 063408
[19] Garcia S, Maxein D, Hohmann L, Reichel J and Long R 2013 *Appl. Phys. Lett.* **103** 114103
[20] Kaufman A M, Lester B J and Regal C A 2012 *Phys. Rev.* X **2** 041014
[21] Thompson J D, Tiecke T G, Zibrov A S, Vuletić V and Lukin M D 2013 *Phys. Rev. Lett.* **110** 133001
[22] Sompet P, Carpentier A V, Fung Y H, McGovern M and Andersen M F 2013 *Phys. Rev.* A **88** 051401
[23] Grünzweig T, Hilliard A, McGovern M and Andersen M F 2010 *Nat. Phys.* **6** 951–4
[24] Arora B, Safronova M and Clark C 2007 *Phys. Rev.* A **76** 052509
[25] McKeever J, Buck J R, Boozer A D, Kuzmich A, Nägerl H C, Stamper-Kurn D M and Kimble H J 2003 *Phys. Rev. Lett.* **90** 133602
[26] Katori H, Ido T and Kuwata-Gonokami M 1999 *J. Phys. Soc. Japan* **68** 2479–82
[27] Savard T, O'Hara K and Thomas J 1997 *Phys. Rev.* A **56** R1095–8
[28] Metcalf H J and van der Straten P 1999 *Laser Cooling and Trapping* (Berlin: Springer) (https://doi.org/10.1007/978-1-4612-1470-0)
[29] Dalibard J and Cohen-Tannoudji C 1989 *J. Opt. Soc. Am.* B **6** 2023